TSINGHUA SCIENCE AND TECHNOLOGY
ISSN 1007-0214 01/16 pp363-376
Volume 15, Number 4, August 2010

Hydrogen Adsorption on Metal-Organic Framework MOF-177

Dipendu Saha, Shuguang Deng**

Chemical Engineering Department, New Mexico State University, Las Cruces, NM 88003, USA

Abstract: This review summarizes the recent literature on the synthesis, characterization, and adsorption properties of meal-organic framework MOF-177. MOF-177 is a porous crystalline material that consists of Zn_4O tetrahedrons connected with benzene tribenzoate (BTB) ligands. It is an ideal adsorbent with an exceptionally high specific surface area (BET>4500 m^2/g), a uniform micropore size distribution with a median pore diameter of 12.7 Å, a large pore volume (2.65 cm^3/g), and very promising adsorption properties for hydrogen storage and other gas separation and purification applications. A hydrogen adsorption amount of 19.6 wt.% on MOF-177 at 77 K and 100 bar was observed, and a CO_2 uptake of 35 mmol/g on MOF-177 was measured at 45 bar and an ambient temperature. Other hydrogen properties (kinetics and heat of adsorption) along with adsorption of other gases including CO_2, CO, CH_4, and N_2O on MOF-177 were also be discussed. It was observed in experiments that MOF-177 adsorbent tends to degrade or decompose when it is exposed to moisture. Thermogravimetric analysis showed that the structure of MOF-177 remains intact at temperatures below 330℃ under a flow of oxygen, but decomposes to zinc oxide at 420℃.

Key words: metal-organic framework; MOF-177; adsorption; hydrogen storage

Introduction

Due to severe environmental impacts and ever-depleted petroleum deposits, petroleum fuels-powered transportation systems desperately need an alternative power source that is clean and sustainable. The proton exchange membrane fuel cell, driven by hydrogen gas, is considered to be one of the feasible energy systems for the future transport systems. There are two ways of storing hydrogen for transportation applications: chemical adsorption and physical adsorption. In chemical adsorption, hydrogen is reversibly and chemically bonded to a substance from that it can be recovered by thermal applications. Typical chemical adsorbents are numerous kinds of metal hydrides[1,2] or aminoboranes[3,4] that have been examined by several researchers for hydrogen storage applications. The main shortcomings of the chemical storage systems are the needs of high temperature for hydrogen desorption and slow desorption kinetics. In the physical adsorption process, the gas molecules are weakly held within the pores of adsorbents material by Van der Waals force, typically stabilizing at low temperatures and high pressures. When the system pressure is lowered or temperature is raised, the adsorbed hydrogen molecules can be readily released. Several porous materials that have been evaluated for hydrogen adsorption include zeolites[5], silica materials[6], and numerous types of carbonaceous materials[7-16].

Most recently, a new type of adsorbents, metal-organic frameworks (MOFs), were synthesized with numerous unique characteristics including extremely high surface area, uniform size distribution with median pore size less than 2 nm, large pore volume and promising adsorption properties for hydrogen storage and gas separation and purifications[17-31]. Metal-organic

Received: 2010-05-19; revised: 2010-07-08

** To whom correspondence should be addressed.
E-mail: sdeng@nmsu.edu; Tel: 01-575-646-4346, Fax: 01-575-646-7706

frameworks, also known as coordination polymers, consist of metal or metal-ion vertices, connected by organic molecules, popularly known as organic linkers. There are numerous varieties of MOFs that have been synthesized using different molecular building blocks but only a fraction of them can be employed for hydrogen storage applications. Metal containing vertices and the organic linker both play the vital role towards chemical functionality or geometric rigidity. The synthetic conditions of MOFs were deliberately designed as mild in order to protect its structural integrity.

Numerous metal-organic frameworks have been synthesized experimentally[17-31] and studied theoretically[32-46] for further modification or for the prediction of novel properties. The metal-organic frameworks are classified as microporous materials as per IUPAC definitions and possess the type-I adsorption isotherm for many gases. In general, MOFs can be classified into two kinds: the zinc-based and other metals-based. Several zinc-based frameworks have been synthesized and examined for hydrogen adsorption. In all the Zn-based MOFs, Zn_4O is used as the metal center and zinc nitrate tetrahydrate is used as the starting chemical to introduce zinc on to the framework. In the family of zinc-based MOFs, the isoreticular metal-organic frameworks or IRMOFs are the most important MOF family members due to their unique structure-property relationships. The word 'isoreticular' originated from the phrase 'same net' that essentially means these are produced with similar technique (mostly solvothermal synthesis) and similar metal clusters by varying the organic linker molecules. Sixteen IRMOFs have been synthesized and reported[47]. A summary of the major IRMOF members and their corresponding organic linker identities are summarized in Table 1[48].

Table 1 Summary of IRMOFs and corresponding organic linkers

IRMOF species	Organic linkers
IRMOF-1 $[Zn_4O(C_8H_4O_4)_3]$	Benzene-1, 4-dicarboxylic acid
IRMOF-2 $[Zn_4O(C_8H_3BrO_4)_3]$	2-bromobenzene-1, 4- dicarboxylic acid
IRMOF-3 $[Zn_4O(C_8H_5NO_4)_3]$	2-aminobenzene-1, 4- dicarboxylic acid
IRMOF-6 $[Zn_4O(C_{10}H_6O_4)_3]$	1, 2-dihydrocyclobutabenzene-3,6- dicarboxylic acid
IRMOF-8 $[Zn_4O(C_{12}H_6O_4)_3]$	Naphthalene-2, 6-dicarboxylic acid
IRMOF-9 $[Zn_4O(C_{12}H_8O_4)_3]$	4, 4' biphenyldicarboxylic acid
IRMOF-11 $[Zn_4O(C_{18}H_{12}O_4)_3]$	4, 5, 9, 10-tetrahydropyrene-2, 7- dicarboxylic acid
IRMOF-13 $Zn_4O(C1_8H_8O_4)_3]$	Pyrene-2, 7-dicarboxylic acid
IRMOF-18 $[Zn_4O(C_{12}H_{12}O_4)_3]$	2, 3, 5, 6-tetramethylbenzene-1, 4-dicarboxylic acid
IRMOF-20 $[Zn_4O(C_8H_2O_4S_2)_3]$	Thieno[3, 2-b]thiophene-2, 5-dicarboxylic acid
MOF-177 $[Zn_4O(C_{27}H_{15}O_6)_3]$	1, 3, 5-tris(4-carboxyphenyl) benzene or benzene tri benzoic acid (BTB)

Apart from zinc, other metals have also been employed to generate MOFs with suitable hydrogen adsorption properties. Light metal tends to reduce framework density thereby increasing gravimetric uptake capacity. Metals that have been studied for MOF synthesis are aluminum (Al)[49,50], copper (Cu)[51-54], chromium (Cr)[55-57], manganese (Mn)[58], iron (Fe)[59], zirconium (Zr)[60], and scandium (Sc)[61].

The ideal pore size of an adsorbent for optimal hydrogen adsorption should be very close to the diameter of a hydrogen molecule (Van der Waals radius of 1.2 Å (1 Å=0.1 nm), kinetic diameter of 2.89 Å). If the pore size is too large, the pore space detracts from the hydrogen molecules; if the pore size is too small, the majority of the pores will not be accessible to hydrogen molecules. Generally speaking, the walls of the adsorbent molecules should be thin and be composed of light elements (like a graphite sheet)[62]. The segmentation of a graphite sheet by an incision of benzene aromatic rings is one way to increase the specific surface area as well as the porosity[63]. One of the key features to shrink the pore size of the MOF is to employ organic linkers of shorter length. However, with shorter linkers, the material may become non-porous due to the increase in framework density (by lowering void space), and gravimetric density decreases. Therefore, the optimal approach must be made between volumetric density and gravimetric uptake of hydrogen.

One approach to optimize the pore size and the

hydrogen volumetric density is to insert guest species in the pores of the MOFs[62]. This approach can be achieved by impregnation with a non-volatile guest or catenation by a similar type of framework. The guest species will not only narrow the pore size of the framework but also provide an additional surface for hydrogen adsorption. It is quite evident that the guest should be lightweight, reactive, large and spindly type of molecules or complexes[62].

Catenation of metal-organic frameworks has long been practiced by researchers for the reduction of free diameters of pores. Catenation can be achieved in two different ways, namely, interpenetration and interweaving. In interpenetration, frameworks are maximally displaced from each other; where in the case of interweaving, the frameworks are minimally displaced along with the exhibition of some close contacts[64]. It is generally argued that interpenetration is more desirable than interweaving[62]. However, interweaving inserts more rigidity to the framework, but it covers the adsorption sites along with increasing in the thickness in the pore wall, thereby increasing its density. Interpenetration decreases the pore volume without blocking the adsorption sites and in most cases it also creates a convoluted pore volume[62].

1 Metal-Organic Framework MOF-177

MOF-5 or IRMOF-1 is the first member of the isoreticular and zinc-based MOF series and numerous research works on MOF-5 have been published[64-81]. Despite a better pore texture and higher adsorption amount for many gases, the number of publications on MOF-177 is much less than that on MOF-5. The first report on experimental synthesis of MOF-177 by Chae et al. was published in 2004[82]. However, the gas adsorption studies on MOF-177 in that work were not reported in detail. In the following years, MOF-177 has attracted different researchers to study its structure-property relationships and gas adsorption properties[48, 82-99].

The typical schematic representation of MOF-177 is shown in Fig. 1[62]. The large yellow sphere is the void space or pore space of the MOF-177 that is partially responsible for the gas adsorption. The Zn_4O clusters are placed at the corners of the framework, connected by organic linker molecules, which are benzenetribezoate

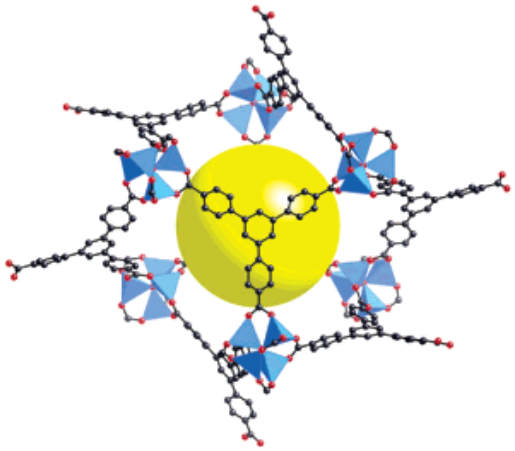

Fig. 1 Schematic diagram of molecular structure of MOF-177[62]

(BTB) for this typical framework (MOF-177).

Besides the pure species of MOF-177, hybrid species of MOF-177 have also been synthesized and reported in the literature[85-87]. Koh et al.[85] synthesized a hybrid species of MOF-5 and MOF-177 by varying the proportions of benzene dicarboxylic acid (BDC) and BTB ligand. They observed that different types of hybrid species were generated at different mole ratios of those two organic linkers. The pure hybrid species, generated at the mole ratio 7:3 to 5:5 of BDC over BTB, is named UMCM-1, where UMCM stands for University of Michigan crystalline material. Table 2 shows the different hybrid species generated at different mole ratios. Saha and Deng[86] also synthesized the hybrid species of MOF-5 and MOF-177, but they did not vary the mole ratio to observe the nature of the hybrid species. In another work, Koh et al.[87] synthesized the hybrid species with organic linkers of BTB ligand and H_2T^2DC and named it UMCM-2, which has a BET specific surface area of more than 5000 m^2/g.

Table 2 Different proportions of BDC and BTB for generating the hybrid species

BDC:BTB	Species generated
10:0-9:1	MOF-5
9:1-7:3	MOF5+ UMCM-1
7:3-5:5	UMCM-1
5:5-4:6	UMCM1+ MOF-177
4:6-0:10	MOF-177

2 Synthesis of MOF-177

Two different pathways of synthesizing MOF-177 have been reported: the solvothermal technique[62,84,88-95] and

the room temperature synthesis[96]. The most common path is the solvothermal synthesis in which the zinc salt and the organic linkers are dissolved in a suitable solvent under suitable heating conditions. On the other hand, in the ambient temperature technique, the constituents were stirred in the solvent for a longer time to obtain the MOF-177 crystals.

In the case of solvothermal synthesis, the reaction time and the type of organic solvents were varied in different works. N, N, diethylformamide (DEF) was incorporated in the work of Furukawa et al.[92], Li and Yang[93] or Caskey et al.[97] However, N, N, methylformamide (DMF) was employed by Saha et al.[88] and Saha and Deng[89-91]. The reaction time for synthesis and some other parameters were slightly different in different published works. The major parameters for synthesizing MOF-177 using the solvothermal technique are summarized in Table 3.

Table 3 Summary of synthesis parameters of the solvothermal technique

Solvent	Solvent purification	Reaction time and temperature	Crystal purification	References
DEF	Not mentioned	100℃/23 h	Not mentioned	Chae et al.[82]
DEF	Not mentioned	85℃/2 d	Chloroform/3 d	Furukawa et al.[92]
DEF	Not mentioned	100℃/23 h and then 23℃/30 d	Chlorobenzene/2 or 24 h (in two batches)	Li and Yang[93]
DEF	Not mentioned	100℃/2 d	Not mentioned	Caskey et al.[97]
DMF	Freeze-pump-thaw method	67℃/7 d	Chloroform/70℃/3 d	Saha et al.[88]
DMF	Freeze-pump-thaw method	70℃/7 d	Chloroform/70℃/3 d	Saha and Deng[89]

The ambient temperature synthesis route for MOF-177 along with some other MOFs was reported by Tranchemontagne et al.[96] In this work, the BTB ligand was stirred with $Zn(OAc)_2$ in DEF solvent for 3 h at room temperature to get the MOF-177 crystals.

Despite the BTB ligand being available commercially; it was synthesized prior to synthesizing MOF-177 in all the published works of MOF-177. There are three different paths of BTB synthesis available in the literature. In the traditional way, the synthesis procedure is composed with two parts. In the first part, 1, 3, 5-triphenyl benzene is converted to 1, 3, 5-acetylated triphenyl benzene with the help of Friedel-kraft acetylation. In the second part, acetylated triphenyl benzene is performed with haloform oxidation to produce BTB. However, the intermediate steps are very complicated[88,92]. In the second way of BTB synthesis, the process begins with 1, 3, 5-tris(4-bromophenyl) benzene that is ultimately converted to BTB with the application of butyllithium, CO_2, and glacial acetic acid[98]. The third path of synthesizing BTB ligand starts with 4-methylacetophenone that is converted to 1, 3, 5-tris(methylphenyl) benzene by the reaction of triflic acid (CF_3SOOH) with toluene under a refluxed condition. Finally, the 1, 3, 5-tris(methylphenyl) benzene resulting from the above reactions is converted to BTB by reacting with HNO_3. The steps for the synthesis of BTB ligand were described in detail in Figs. 2a, 2b, 3, and 4.

3 Material Characterization

3.1 Pore textural properties of MOF-177

The very high surface area and large pore volume are the main attractive features of MOF-177. The Langmuir specific surface area of this adsorbent varies from 4300 m^2/g[93] to 5994 m^2/g[88], and the BET specific surface area varied from 3275 m^2/g[88] to 4630 m^2/g[92]. The median pore diameter recorded in the microporous region are between 10.6 Å[82] and 12.7 Å[88]. Pore volume was recorded as high as 2.65 cm^3/g by Saha et al.[88], which is probably the largest pore volume of any kind of adsorbent ever reported. Table 4 summarizes the pore textural properties of MOF-177 reported by different researchers.

3.2 XRD patterns

The major peaks in the XRD patterns of MOF-177 reported in different publications are quite consistent. However, the peak positions and the location of the strongest peak are shifted to a small extent. The main peaks of the pattern appear in the $4.395° < 2\theta < 41.661°$[82], which remained identical in almost works. In the work of Saha et al.[88], the main peaks at 4.7°, 6.2°, 10.1°, and 13.5° are well identified. However, in the work by Li and Yang[93] the largest peak appeared at around 5°, unlike the pattern generated by Rowsell's dissertation[48] (around 6°) or by work by Saha et al.[88]

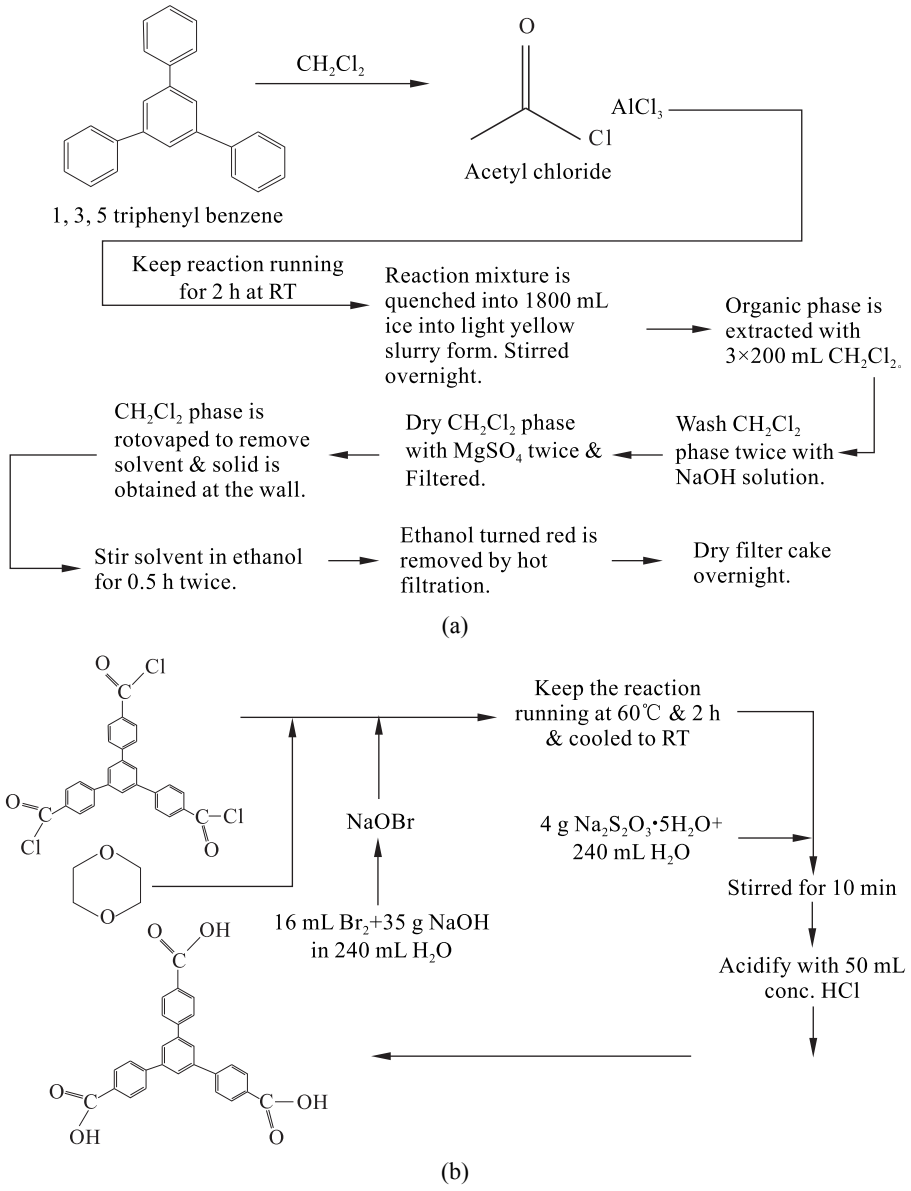

Fig. 2 (a) Acetylation steps of 1, 3, 5-triphenyl benzene, and (b) Conversion of acetylated triphenyl benzene to BTB

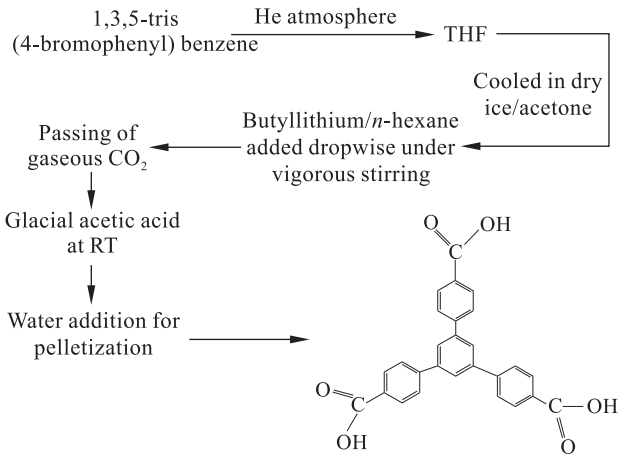

Fig. 3 Synthesis of BTB from 1, 3, 5-tris(4-bromophenyl) benzene

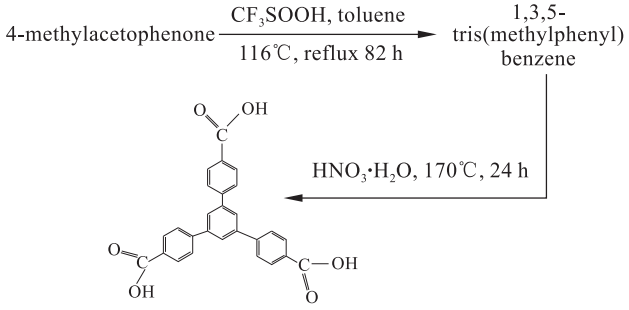

Fig. 4 Synthesis BTB ligand from 4-methylacetophenone

Table 4 Summary of pore textural properties of MOF-177

Langmuir surface area (m^2/g)	BET surface area (m^2/g)	Pore width (Å)	Pore volume (cm^3/g)	References
4500	–	10.80	1.59	Chae et al.[82]
5250	4630	–	1.56	Furukawa et al.[92]
4508	–	11.17	–	Millward and Yaghi[94]
5640	–	–	–	Wong-Foy et al.[95]
4300	3100	10.60	–	Li and Yang[93]
5994	3275	12.70	2.65	Saha et al.[88]

(4.7°). There are also existing differences in the locations of the smaller peaks. Most probably, the different reaction (crystallization) conditions caused these differences in the peaks. According to the work by Chae et al.[82], the crystals of MOF-177 was indexed with trigonal type with a space group P31c (163) and lattice parameters a=31.072 Å, c=30.0332 Å. However, in the work by Saha et al.[88], the crystal was indexed with hexagonal P63 (173) and cell parameters, $a=b=$ 20.905 Å, c=22.718 Å, $\alpha=\beta$=90°, γ=120°.

3.3 SEM images

The SEM images of MOF-177 that appeared only in the work by Li and Yang[93], Saha et al.[88], and Li et al.[98] are shown in Figs. 5, 6, and 7. It can be observed from the work of Saha et al.[88] and Li and Yang[93], the definite crystal shape is not observed, most probably due to the polycrystalline agglomerate nature of the crystals. However, in the work of Li et al.[98], a definite crystal shape is observed at particular reaction conditions.

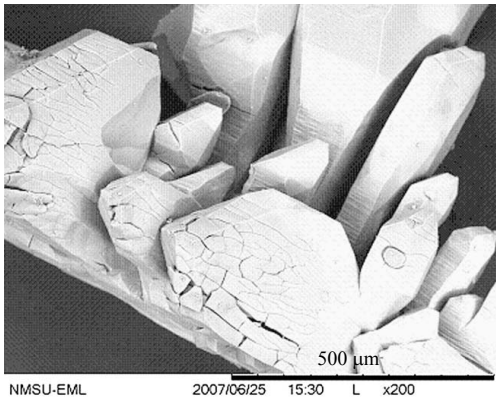

(a)

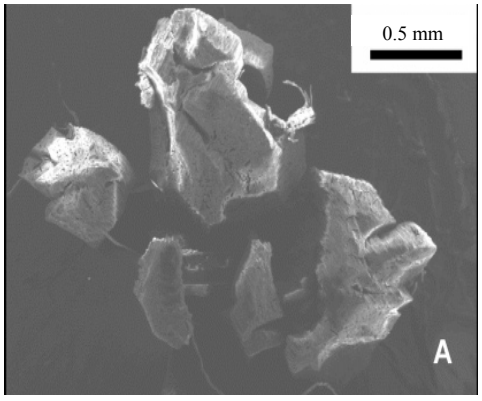

(b)

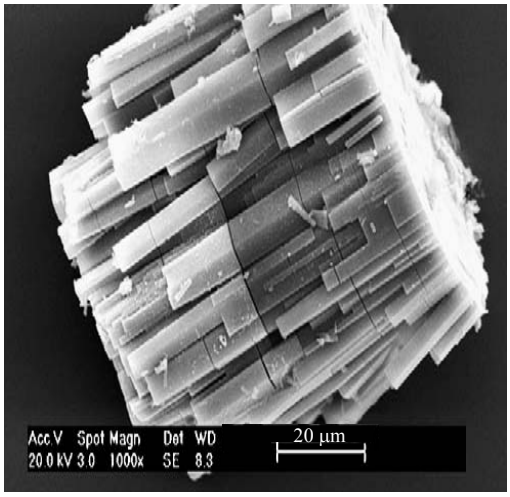

(c)

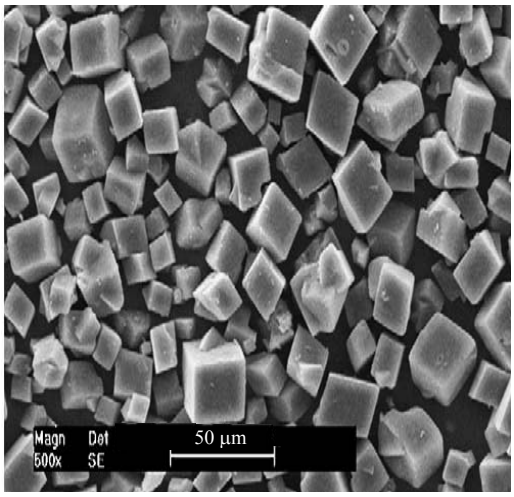

(d)

Fig. 5 (a) SEM image of MOF-177 reported by Saha et al.[88], (b) SEM image of MOF-177 reported by Li and Yang[93], and (c) and (d) SEM images of MOF-177 reported by Li et al.[98]

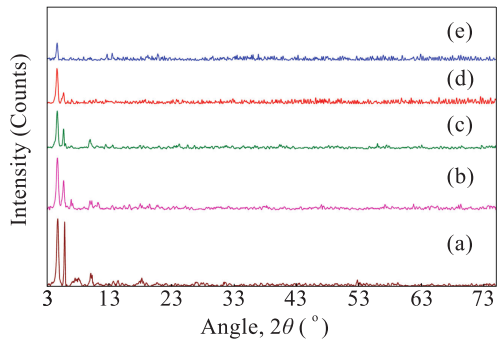

Fig. 6 Gradual shift of XRD patterns after MOF-177 is exposed to moist air[89].

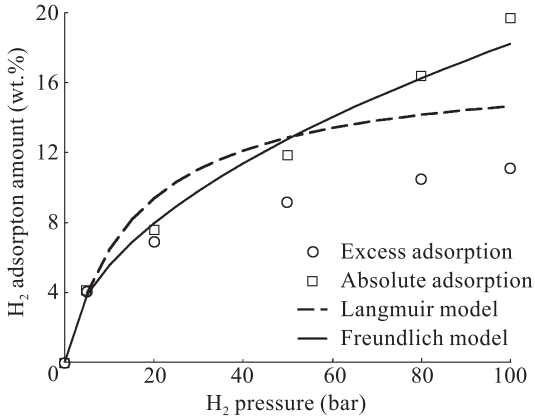

Fig. 7 Adsorption isotherm of hydrogen on MOF-177 at 77 K[88]

3.4 Structural stability study

Similar to the other members of isoreticular metal-organic framework series, the framework structure of MOF-177 is highly vulnerable to water. The structure collapses even if MOF-177 is exposed to moist air for some time period. Though this observation was mentioned in the work by Li and Yang[93], the detailed investigation was reported in the work of Saha and Deng[89]. In their work, MOF-177 sample was exposed to ambient air at relative humidity of 16% for 5 weeks and monitored for its structural changes by XRD. The crystal structure of MOF-177 gradually changed from hexagonal to orthogonal in first week, and then to monoclinic in the total 5 week period. The crystal structure of MOF-177 was completely destroyed after it is immersed in water. The detailed crystallographic information of structural decay is revealed in Table 5[89] and gradual shifting of XRD peaks is shown in Fig. 6[89].

Based on the possible reaction mechanism of structural decay shown by Greathouse and Allendrof[99] for MOF-5, Li and Yang[93] and Saha et al.[88] has shown the possible reaction mechanism of interaction of MOF-177 with water.

Table 5 Summary of chronological structural property changes of a MOF-177 sample

	Cell type	Space group	Lattice parameter (Å)			Lattice angle (°)			Cell volume (Å^3)
			a	*b*	*c*	*α*	*β*	*γ*	
Fresh sample	Hexagonal	P63(173)	20.905	20.905	22.718	90°	90.0°	120°	8598.4
After 1 week	Orthogonal	Pbam(55)	19.161	23.691	17.527	90°	90.0°	90°	7956.5
After 2 weeks	Monoclinic	P2/c (13)	18.700	17.870	21.540	90°	123.2°	90°	6025.8
After 3 weeks	Monoclinic	P2/c(13)	18.878	15.307	18.947	90°	97.7°	90°	5425.2
After 4 weeks	Monoclinic	P21(4)	18.641	16.223	23.724	90°	138.7°	90°	4739.1
After 5 weeks	Monoclinic	P2/m(10)	19.874	13.066	24.785	90°	114.0°	90°	5879.9

$$Zn_4O(BTB)_2+4H_2O\rightarrow[(Zn_4O)(H_2O)_4(BTB)]^{3+}+BTB^{3-} \quad (1)$$

$$[(Zn_4O)(H_2O)_4(BTB)]^{3+}\rightarrow Zn(OH)_2+3ZnO+BTB(3H)+3H^+ \quad (2)$$

In the thermogravimetric analysis made by Saha and Deng[89], it was observed that the weight loss of MOF-177 is negligible at temperatures below 330℃ in the presence of oxygen or vacuum. However, MOF-177 completely converts to zinc oxide at 420℃ in either condition.

4 Adsorption Properties

4.1 Hydrogen adsorption

4.1.1 Hydrogen adsorption at low pressures

The majority of the published works on MOF-177 dealt with hydrogen adsorption research. In the ambient pressure region, five different temperatures have been employed to examine the hydrogen adsorption capacity, 77 K, 87 K, 194.5 K, 298 K, and 323 K[88,93].

The highest H_2 uptake was reported by 1.45 wt.% at 77 K by Li and Yang[93] The detailed hydrogen uptake amounts in various temperatures and an ambient pressure were summarized in Table 6.

Table 6 Hydrogen adsorption capacity of MOF-177 at ambient pressure

Temperature (K)	Uptake amount	Reference
77.0	75 mg/g	Furukawa et al.[92]
87.0	13 mg/g	
77.0	1.25 wt.%	Rowsell[48]
77.0	1.45 wt.%	Li and Yang[93]
273.0	2.3 cm^3/g	
298.0	1.8 cm^3/g	
323.0	1.5 cm^3/g	
77.0	1.36 wt.%	Saha et al.[88]
194.5	0.92 wt.%	
298.0	0.012 wt.%	

4.1.2 Hydrogen adsorption at high pressures

In the adsorption experiments at a high pressure region, three different temperatures have been reported, 50 K, 77 K, and ambient temperature. Wong-Foy et al.[95] reported 75 mg/g excess hydrogen adsorption at 77 K and 90 bar pressure. An excess hydrogen adsorption amount of 80 mg/g corresponding to 120 mg/g of absolute adsorption was observed in the work of Furukawa et al. at 80 bar and 77 K[92]. The highest hydrogen adsorption was reported in the work of Saha et al.[88] at 77 K and 100 bar (19.6 wt.% absolute adsorption). The hydrogen adsorption isotherm at 77 K and pressure up to 100 bar is shown in Fig. 7. Similar to the other types of MOFs, the hydrogen uptake at ambient temperatures is also quite low for MOF-177, 0.35 wt.% at 40 bar and 298 K[88] and 0.6 wt.% at 100 bar and 298 K[93].

Isotherm modeling with Freundlich and Langmuir equations was reported by Saha et al.[88] It was observed that Freundlich equation better fits the experimental points. Poirrer and Dailly[100] modeled the excess isotherm parameters using Dubinin-Astakov (DA) models. Table 7a shows the isotherm model parameter values for Langmuir and Freundlich equation[88] and Table 7b lists the model parameter values for the DA equation[100]. The values inside and outside the parenthesis of Table 7b correspond to the calculations based on the pressure and fugacity.

Table 7a Langmuir and Freundlich model parameter values[88]

T/K	Langmuir		Freundlich	Parameters
	a_m (wt.%)	b (bar^{-1})	k	n
77 (low pressure)	1.80	1.35	1.34	1.40
194.5 (low pressure)	14.80	0.07	0.93	0.99
297 (low pressure)	–	–	0.05	0.56
77 (High pressure)	17.00	0.06	1.71	1.95
297 (High pressure)	0.70	0.02	0.03	1.39

Table 7b DA equation model parameter values[99]

Parameter name	Parameter values	Standard error
W_0 (mL/g)	2.28 (2.40)	±0.09
E (J/mol)	1869 (1842)	±30
m	1.68 (1.64)	±0.05
γ	2.48 (2.50)	±0.1
α	0.0054 (0.0049)	±0.0007
ρ_a	0.056 (0.054)	± 0.001

The difference in hydrogen adsorption is most probably attributed to the slight difference in crystalline properties which in turn is monitored by the synthesis conditions. The XRD pattern of MOF-177 shown by Saha et al.[88] is slightly different from Li and Yang[93] or Chae et al.[82] which is also further confirmed by the different crystal type and space group by two research groups. Most probably the solvent degassing and prolong heating with lower temperature during the synthesis caused the different types of crystals with higher pore volume resulting in better gas uptake. The methods of degassing before the gas adsorption measurement might also affect the hydrogen gas uptake in a smaller extent.

4.1.3 Increased hydrogen adsorption by spill-over

One of the promising ways of increasing the hydrogen uptake at ambient temperatures is to dope the adsorbent with certain types of transition metals, like palladium (Pd), platinum (Pt), nickel (Ni) or ruthenium (Ru)[8]. The metal sites are known to dissociate the adsorbed hydrogen molecules and to facilitate hydrogen adsorption on the internal pore surfaces of the host support through the spillover phenomenon[69-73]. Li and Yang[93] mixed platinum doped activated carbon with MOF-177 that resulted in 0.78 wt.% of hydrogen adsorption at 298 K temperature and 100 bar pressure. However, when they bridged the Pt/activated carbon with MOF-177 with carbonized sucrose to facilitate the surface diffusion, the hydrogen uptake increased to 1.4 wt.% at 100 bar and 298 K temperature.

4.1.4 Hydrogen adsorption kinetics

The adsorption kinetics of hydrogen on MOF-177 is as important as the hydrogen adsorption amount because the adsorption kinetics determine how fast hydrogen is adsorbed or desorbed in the storage system. Saha et al.[88] performed a detailed kinetic study of hydrogen adsorption on MOF-177. In order to describe the adsorption kinetics and to determine the intracrystalline diffusivity of hydrogen in MOF-5 crystals, a pore diffusion model was derived to correlate the hydrogen adsorption kinetic data following Ruthven[101]. By neglecting the heat transfer between particle and surrounding fluid, the diffusion equation in spherical coordinates is written as[101]

$$\frac{\partial q}{\partial t}=\frac{1}{r^2}\frac{\partial}{\partial r}\left(r^2 D_{\mathrm{c}}\frac{\partial q}{\partial r}\right) \tag{3}$$

where r is the radius of the equivalent sphere, D_{c} is the intracrystalline diffusivity and $q(r, t)$ is the adsorbed amount at time t and radial position r. For constant diffusivity at a given particular pressure, Eq. (3) can be converted to

$$\frac{\partial q}{\partial t}=D_{\mathrm{c}}\left(\frac{\partial^2 q}{\partial r^2}+\frac{2}{r}\frac{\partial q}{\partial r}\right) \tag{4}$$

The solution of Eq. (4) is given by

$$\frac{\bar{q}-q_0'}{q_0-q_0'}=\frac{m_t}{m_\infty}=1-\frac{6}{\pi^2}\sum_{n=1}^{\infty}\frac{1}{n^2}\exp\left(\frac{-\pi^2 D_{\mathrm{c}} t}{r_{\mathrm{c}}^2}\right) \tag{5}$$

where, $\bar{q}$ (wt.%) is the average adsorbate concentration in the particle, q_0' is the initial adsorbate concentration in the adsorbent particle (wt.%), q_0 is the equilibrium adsorbate concentration in the adsorbent particle (wt.%), r_{c} is the equivalent sphere radius of adsorbent particle, and (m_t/m_∞) is the fractional adsorption uptake.

For fractional uptake (m_t/m_∞) greater than 70%, Eq. (5) can be reduced to the following equation with less than 2% error.

$$1-\frac{m_t}{m_\infty}\approx\frac{6}{\pi^2}\exp\left(\frac{-\pi^2 D_{\mathrm{c}} t}{r_{\mathrm{c}}^2}\right) \tag{6}$$

In the study of Saha et al.[88], Eq. (6) was used as the diffusion model equation to correlate the hydrogen adsorption kinetic data. Only data points with (m_t/m_∞) greater than 70% and less than 99% were used for estimating the diffusivities. It was observed that the average diffusion time constant (s^{-1}) of H_2 on MOF-177 is 0.0964, 0.2140, and 0.3023 at 77 K, 194.5 K, and 298 K, respectively. It was also observed that diffusion time constant increases with increasing pressure and temperature.

4.1.5 Activation energy of hydrogen adsorption

The activation energy for hydrogen diffusion can be estimated from the Eyring equation by assuming hydrogen diffusion inside MOF-177 to be an activation process. The Eyring equation is given by

$$D_{\mathrm{c}}=D_{\mathrm{c0}}\exp\left(-\frac{E}{RT}\right) \tag{7}$$

where D_{c0} is an equation constant, E is the activation energy for diffusion. Saha et al.[88] found that the activation energy for hydrogen diffusion in MOF-177 is 0.94 kJ/mol, which is much smaller as compared with the activation energy for small hydrocarbon molecules diffusion in zeolite[101].

4.1.6 Heat of adsorption of hydrogen on MOF-177

The heat of adsorption is an important measure for determining the adsorbate-adsorbent interactions. In general, the heat of adsorption is very low for all the metal-organic frameworks that are the cause of the poor adsorption amount at ambient temperature conditions. It was observed the heat of adsorption lies within –4 to –7 kJ/mol for most of the metal-organic frameworks[59,61]. Higher heat of adsorption was reported for MIL-101, which was about –9.3 to –10 kJ/mol[59,102]. Saha et al.[88] reported the heat of adsorption of MOF-177 to be 4 to 0.1 kJ/mol within 0 to 1 wt.% of hydrogen adsorption. Li and Yang[93] reported the highest of heat of adsorption of 11.3 kJ/mol to 5.8 kJ/mol within the adsorption amount of 0.32 to 1.5 cm^3/g. Recently, Poirrer and Daily[100] reported

heat of adsorption values of 3-5 kJ/mol within the fractional filling of 0.2 to 0.9.

4.2 Adsorption of other gases

The adsorption of CO_2 on MOF-177 has also been extensively studied because MOF-177 is considered to be the most promising adsorbent for CO_2 storage and separation. Millward and Yaghi[94] reported a CO_2 uptake as high as 35 mmol/g at 45 bar and an ambient temperature. Saha and Deng[91] reported 0.18 and 9.09 mmol/g CO_2 adsorption at 298 K and 1 bar and 14 bar, respectively. They also reported the selectivity of CO_2/N_2 and CO_2/CH_4 to be 17.73 and 4.43 respectively[91]. CO adsorption study on MOF-177 was also performed by Saha and Deng[90] along with MOF-5 and zeolite 5A at 194.5 K, 237 K, and 194.5 K and at 1 bar pressure. It was observed that MOF-177 can adsorb 4.6 mmol/g of CO at 194.5 K and 1 bar. It was also observed that the average diffusivity of CO on MOF-177 is 5.01×10^{-9} m^2/s at 298 K and the diffusivity decreases with adsorbate pressure. The heat of CO adsorption on MOF-177 was estimated to be 19-21 kJ/mol. Adsorption of CH_4 and N_2O on MOF-177, MOF-5, and zeolite 5A was also performed by Saha and Deng[91] and it was observed that CH_4 and N_2O adsorption uptakes were 0.98 and 0.2 wt.% at 298 K and 1 bar. The average diffusivities of CO_2, CH_4, and N_2O in MOF-177 were also calculated. The adsorption amounts and diffusivities of CO_2, CO, CH_4, and N_2O on MOF-177 are summarized in Table 8.

Table 8 CO_2, CO, CH_4, and N_2O adsorption properties of MOF-177

Gas	Low pressure uptake (P=1 bar, T=298 K)	Low pressure uptake (P=1 bar, T=237 K)	Low pressure uptake (P=1 bar, T=194.5 K)	High pressure uptake (T=298 K)	Average diffusivity (m^2/s)	References
CO_2	7 wt.%	–	–	9.09 mmol/g (P=14 bar)	2.3×10^{-9}	Saha and Deng[91]
	–	–	–	35 mmol/g (P=45 bar)	…	Millward and Yaghi[94]
CO	0.2 mmol/g	3 mmol/g	4.6 mmol/g	–	5.01×10^{-9}	Saha and Deng[90]
CH_4	0.98 wt.%	–	–	22 wt.% (P=100 bar)	1.46×10^{-9}	Saha and Deng[91]
N_2O	0.2 wt.%	–	–	–	1.09×10^{-9}	Saha and Deng[91]

5 Concluding Remarks

A brief review of recent publications on synthesis, characterization, and adsorption properties of metal-organic framework MOF-177 was presented in this article. MOF-177 appears to be a very promising new adsorbent with unique pore textural properties (Langmuir specific area: 4508-5996 m^2/g, BET specific area: 3100-4630 m^2/g, pore size: 10.6-12.7 Å, pore volume: 2.65 cm^3/g) and excellent adsorption properties for hydrogen and carbon dioxide. The hydrogen adsorption amount of 19.6 wt.% on MOF-177 at 77 K and 100 bar is the highest hydrogen adsorption capacity ever reported on any physical adsorbent. A CO_2 uptake of 35 mmol/g on MOF-177 was measured at 45 bar and an ambient temperature. MOF-177 also has good adsorption properties for other gases including CH_4, CO, and N_2O. The MOF-177 structure is stable in the air at ambient conditions without moisture, but it is very susceptible to water.

Although it was demonstrated that MOF-177 has very promising pore textural and adsorption properties for hydrogen and other gases, MOF-177 is still a model adsorbent being studied in lab research; significant advances in materials production and stability improvement have to be made before it can be used in commercial applications. Because the hydrogen adsorption amount of 19.6 wt.% on MOF-177 was measured at 77 K and 100 bar, this value still does not meet the US Department of Energy (DOE) target of hydrogen storage for fuel cells to be used in transportation. The hydrogen storage capacity on MOF-177 at ambient temperatures and moderate pressures is quite small due to very weak interactions between hydrogen and the MOF-177. Another drawback of the MOF-177 (or basically IRMOFs) is the sensitivity to the moisture. Many MOFs suffer irreversible damages at above 4% moisture level, which also makes it quite difficult to handle in large quantities for commercial applications. Thorough research is needed to convert the IRMOFs hydrophobic and make it easier to handle. The BTB ligand and other chemicals used in MOF-177 synthesis are quite expensive. Alternative synthesis routes to cut the cost for producing MOF-177 are also necessary

before this promising adsorbent can be commercialized.

References

[1] Rangel C M, Fernandes V R, Slavkou Y, et al. Novel hydrogen generator/storage based on metal hydrides. *Int. J. Hydrogen Energ.*, 2009, **34**: 4587-4591.

[2] Schlapbach L, Züttel A. Hydrogen-storage materials for mobile applications. *Nature*, 2001, **414**: 353-358.

[3] Stephens F H, Pons V, Baker R T. Ammonia-borane: The hydrogen storage source par excellence? *Dalton Trans*., 2007, 2613-2626. DOI: 10.103916703053C.

[4] Pons V, Baker R T, Szymczak N K, et al. Coordination of aminoborane, NH_2BH_2, dictates selectivity and extent of H_2 release in metal-catalysed ammonia borane dehydrogenation. *Chem. Comm*., 2008, **48**: 6597-6599.

[5] Weitkamp J, Fritz M, Ernst S. Zeolites as media for hydrogen storage. *Intl. J. Hydrogen Energy*, 1995, **20**: 967-970.

[6] Lan J, Cheng D, Cao D, et al. Silicon nanotube as a promising candidate for hydrogen storage: From the first principle calculations to grand canonical Monte Carlo simulations. *J. Phys. Chem. C*, 2008, **112**: 5598-5604.

[7] Saha D, Wei Z, Velluri S H, et al. Hydrogen adsorption in ordred mesoporous carbon synthesized by soft-template approach. *J. Porous Media*, 2010, **13**: 39-50.

[8] Saha D, Deng S. Hydrogen adsorption on ordered mesoporous carbons doped with Pd, Pt, Ni, and Ru. *Langmuir*, 2009, **25**: 12 550-12 560.

[9] Hirscher M, Bechar M. Hydrogen storage in carbon nanotubes. *J. Nanosci. Nanotechnol*., 2003, **3**: 3-17.

[10] Mandoki M T, Dentzer J, Piquero T, et al. Hydrogen storage in activated carbon materials: Role of the nanoporous texture. *Carbon*, 2004, **42**: 2744-7274.

[11] Anson A, Callejas M A, Benito A M, et al. Hydrogen adsorption studies in single wall carbon nanotubes. *Carbon*, 2004, **42**: 1243-1248.

[12] Liu C, Fan Y Y, Liu M, et al. Hydrogen storage in single-walled carbon nanotubes at room temperature. *Science*, 1999, **286**(5442): 1127-1129.

[13] Shao X, Wang W, Xue R, et al. Adsorption of methane and hydrogen on mesocarbon microbeads by experiment and molecular simulation. *J. Phys. Chem. B*, 2004, **108**: 2970-2978.

[14] Gadiou R, Saadallah S E, Piquero T, et al. The influence of textural properties of hydrogen on ordered nanostructured carbons. *Micropor. Mesepor. Mater*., 2005, **79**: 121-128.

[15] Armandi M, Bonelli B, Bottero I, et al. Synthesis and characterization of ordered porous carbons with potential applications as hydrogen storage media. *Micropor. Mesepor. Mater*., 2007, **103**: 150-157.

[16] Seok Kim H, Singer J P, Gogotsi Y, et al. Molybdenum carbide-derived carbon for hydrogen storage. *Microporous Mesoporous Mater*., 2009, **3**: 267-271.

[17] Rosi N L, Eddaoudi M, Kim J, et al. Infinite secondary building units and forbidden catenation in metal-organic frameworks. *Angew. Chem. Int. Ed*., 2002, **41**: 284-287.

[18] Kitaura R, Onoyama G, Sakamoto H, et al. Immobilization of a Metallo Schiff base into a microporous coordination polymer. *Angew. Chem. Int. Ed*., 2004, **43**: 2684-2687.

[19] Forster P M, Eckert J, Chang J S, et al. Hydrogen adsorption in nanoporous nickel (II) phosphates. *J. Am. Chem. Soc*., 2003, **125**: 1309-1311.

[20] Rowsell J L C, Millward A R, Park K S, et al. Hydrogen sorption in functionalized metal-organic frameworks. *J. Am. Chem. Soc*., 2004, **126**: 5666-5667.

[21] Rosi N L, Eckert J, Eddaoudi M, et al. Hydrogen storage in microporous metal-organic frameworks. *Science*, 2003, **300**: 1127-1129.

[22] Pan L, Sander M B, Huang X, et al. Microporous metal organic materials: Promising candidates as sorbents for hydrogen storage. *J. Am. Chem. Soc*., 2004, **126**: 1308-1309.

[23] Eddaoudi M, Kim J, Rosi N, et al. Systematic design of pore size and functionality in isoreticular metal-organic frameworks and application in methane storage. *Science*, 2002, **295**: 469-472.

[24] Loiseau T, Serre C, Huguenard C, et al. A rationale for the large breathing of the porous aluminum terephthalate (MIL-53) upon hydration. *Chem. Eur. J*., 2004, **10**: 1373-1382.

[25] Dybtsev D N, Chun H, Yoon S H, et al. Microporous manganese formate: A simple metal-organic porous material with high framework stability and highly selective gas sorption properties. *J. Am. Chem. Soc*., 2004, **126**: 32-33.

[26] Lee E Y, Suh M P. A robust porous material constructed of linear coordination polymer chains: Reversible single-crystal to single-crystal transformations upon dehydration and rehydration. *Angew Chem. Int. Ed*., 2004, **43**: 2798-2801.

[27] Dybtsev D N, Chun H, Kim K. Rigid and flexible: A highly porous metal-organic framework with unusual guest-dependent dynamic behavior. *Angew. Chem. Int. Ed.*, 2004, **43**: 5033-5036.

[28] Zhao X, Xiao B, Fletcher A J, et al. Hysteretic adsorption

and desorption of hydrogen by nanoporous metal-organic frameworks. *Science*, 2004, **306**(5698): 1012-1015.

[29] Kesanli Y, Cui M, Smith R, et al. Highly interpenetrated metal-organic frameworks for hydrogen storage. *Angew. Chem. Int. Ed*., 2005, **44**: 72-75.

[30] Kubota Y, Takata M, Matsuda R, et al. Direct observation of hydrogen molecules adsorbed onto a microporous coordination polymer. *Angew. Chem. Int. Ed*., 2004, **117**(6): 942-945.

[31] Chen B, Ockwig N W, Millward A R, et al. High H_2 adsorption in a microporous metal-organic framework with open metal sites. *Angew. Chem. Int. Ed.*, 2005, **44**: 4745-4749.

[32] Lee T B, Jung D H, Kim D, et al. Molecular dynamics simulation study on the hydrogen adsorption and diffusion in non-interpenetrating and interpenetrating IRMOFs. *Catalysis Today*, 146, **1**: 216-222.

[33] Frost H, Snurr R Q. Design requirements for metal-organic frameworks as hydrogen storage materials. *J. Phys. Chem. C*, 2007, **111**: 18 794-18 803.

[34] Walton, Snurr R Q. Applicability of the BET method for determining surface areas of microporous metal-organic frameworks. *J. Am. Chem. Soc.*, 2007, **129**: 8552-8556.

[35] Amirjalayer S, Tafipolsky M, Schmid R. Molecular dynamics simulation of benzene diffusion in MOF-5: Importance of lattice dynamics. *Angew. Chem. Intl. Ed.*, 2007, **46**: 463-466.

[36] Farrusseng D, Daniel C, Gaudillre C, et al. Heats of adsorption for seven gases in three metal-organic frameworks: Systematic comparison of experiment and simulation. *Langmuir*, 2009, **25**(13): 7383-7388.

[37] Liu B, Yang Q, Xue C, et al. Molecular simulation of hydrogen diffusion in interpenetrated metal-organic frameworks. *Phys. Chem. Chem. Phys.*, 2008, **10**: 3244-3249.

[38] Klontzas E, Mavrandonakis A, Tylianakis E, et al. Improving hydrogen storage capacity of MOF by functionalization of the organic linker with lithium atoms. *Nano Lett.*, 2008, **8**: 1572-1576.

[39] Han S S, Soo S, Goddard W A, III. High H_2 storage of hexagonal metal-organic frameworks. *Journal of Physical Chemistry C*, 2008, **112**: 13 431-13 436.

[40] Frost H, Düren T, Snurr R Q. Effects of surface area, free volume, and heat of adsorption on hydrogen uptake in metal-organic frameworks. *J. Phys. Chem. B*, 2006, **110**: 9565-9570.

[41] Huang B L, McGaughey A J H, Kaviany M. Thermal conductivity of metal-organic framework 5 (MOF-5): Part I. Molecular dynamics simulations. *Intl. J. Heat Mass Transfer*, 2007, **3**: 393-404.

[42] Lamia N, Jorge M, Granato M A, et al. Adsorption of propane, propylene and isobutane on a metal-organic framework: Molecular simulation and experiment. *Chemical Eng. Sc*., 2009, **64**(14): 3246-3259.

[43] Karra J R, Walton K S. Effect of open metal sites on adsorption of polar and nonpolar molecules in metal-organic framework Cu-BTC. *Langmuir*, 2008, **24**: 8620-8626.

[44] WaltonK S, Millward A R, Dubbeldam D, et al. Understanding inflections and steps in carbon dioxide adsorption isotherms in metal-organic frameworks. *J. Am. Chem. Soc.*, 2008, **130**: 406-407.

[45] Yang Q, Zhong C. Molecular simulation of carbon dioxide/methane/hydrogen mixture adsorption in metal-organic frameworks. *J. Phys. Chem. B*, 2006, **110**: 17 776-17 783.

[46] Liu Y, Liu H, Hu Y, et al. Development of a density functional theory in three-dimensional nanoconfined space: H_2 storage in metal-organic frameworks. *J. Phys. Chem. B*, 2009, **113**: 12 326-12 331.

[47] Sing K S W, Everett D H, Haul R A W, et al. Reporting physisorption data for gas/solid systems with special reference to the determination of surface area and porosity. *Pure Appl. Chem*., 1985, **57**: 603-619.

[48] Rowsell J L C. Hydrogen storage in metal-organic frameworks: An investigation of structure-property relationships [Dissertation]. Univ. Michigan, USA, 2005: 46-50.

[49] Loiseau T, Lecroq L, Volkringer C, et al. MIL-96, a porous aluminum trimesate 3D structure constructed from a hexagonal network of 18 membered rings and m3-Oxo-centered trinuclear units. *J. Am. Chem. Soc.*, 2006, **128**: 10 223-10 230.

[50] Meilikhov M, Yusenko K, Fischr R A. Turning MIL 53(Al) redox-active by functionalization of the bridging OH-group with 1, 1′ ferrocenediyl-dimethylsilane. *J. Am. Soc.*, 2009, **131**: 9644-9645.

[51] Wang Q M, Shen D, B€ulow M, et al. Metal-organic molecular sieve for gas separation and purification. *Microporous Mesoporous Mater*., 2002, **55**: 217-230.

[52] Keskin S, Liu J, Johnson J K, et al. Testing the accuracy of correlations for multicomponent mass transport of adsorbed gases in metal-organic frameworks: Diffusion of H_2/CH_4 mixtures in CuBTC. *Langmuir*, 2008, **24**: 8254-8261.

[53] Liang Z, Marshall M, Chaffee A L. CO_2 adsorption-based separation by metal organic framework (Cu-BTC) versus zeolite (13X). *Energy & Fuels*, 2009, **23**: 2785-2789.

[54] Rowsell J L C, Yaghi O M. Effects of functionalization, catenation, and variation of the metal oxide and organic linking units on the low-pressure hydrogen adsorption properties of metal-organic frameworks. *J. Am. Soc*., 2006, **128**: 1304-1315.

[55] Serre C, Millange F, Thouvenot C, et al. Very large breathing effect in the first nanoporous chromium (III)-based solids: MIL-53 or Cr^{III} (OH). $\{O_2C\text{-}C_6H_4CO_2\}.\{HO_2C\text{-}C_6H_4\text{-}CO_2H\}x.H_2Oy$. *J. Am. Soc.*, 2002, **124**: 13 519-13 526.

[56] Coudert F X, Mellot-Draznieks C, Fuchs A H, et al. Double structural transition in hybrid material MIL-53 upon hydrocarbon adsorption: The thermodynamics behind the scenes. *J. Am. Soc.*, 2009, **131**: 3442-3443.

[57] Hamon L, Llewellyn P L, Devic T, et al. Co adsorption and separation of CO_2-CH_4 mixtures in the highly flexible MIL 53(Cr) MOF. *J. Am. Soc.*, 2009, **131**: 17 490-17 499.

[58] Dinca M, Daily A, Liu Y, et al. Hydrogen storage in a microporous metal-organic framework with Mn^{2+} coordination sites. *J. Am. Chem. Soc*., 2006, **128**: 16 876-16 883.

[59] Llewellyn P L, Horcajada P, Maurin G, et al. Complex adsorption of short linear alkanes in the flexible metal-organic-framework MIL-53(Fe). *J. Am. Soc.*, 2009, **131**: 13 002-13 008.

[60] Cavka J H, Jakobsen S, Olsbye U, et al. A new zirconium inorganic building brick forming metal organic frameworks with exceptional stability. *J. Am. Chem. Soc.*, 2008, **130**: 13 850-13 851.

[61] Miller S R, Wright P A, Devic T, et al. Single crystal X-ray diffraction studies of carbon dioxide and fuel-related gases adsorbed on the small pore scandium terephthalate metal organic framework, $Sc_2(O_2CC_6H_4CO_2)_3$. *Langmuir*, 2009, **25**: 3618-3626.

[62] Rowsell J L C, Yaghi O M. Strategies for hydrogen storage in metal-organic frameworks. *Angew. Chem. Int. Ed*., 2005, **44**: 4670-4679.

[63] Batten S R, Robson R. Interpenetrating nets: Ordered, periodic entanglement. *Angew. Chem. Int. Ed.*, 1998, **37**: 1460-1494.

[64] Li H, Eddaoudi M, O'Keeffe M, et al. Design and synthesis of an exceptionally stable and highly porous metal-organic framework. *Nature*, 1999, **402**: 276-279.

[65] Saha D, Yang Z, Deng S. Hydrogen adsorption on metal-organic framework (MOF-5) synthesized by DMF approach. *J. Porous Materials*, 2009, **16**: 141-149.

[66] Saha D, Wei Z, Deng S. Hydrogen adsorption equilibrium and kinetics in metal-organic framework (MOF-5) synthesized with DEF approach. *Separation Purification Technol.*, 2009, **64**: 280-287.

[67] Panella B, Hirscher M. Hydrogen physiosorption in metal-organic porous crustals. *Adv. Mater.*, 2005, **17**: 538-541.

[68] Kaye S S, Daily A, Yaghi O M, et al. Impact of preparation and handling on the hydrogen storage properties of Zn_4O (1,4-benzenedicarboxylate)$_3$ (MOF-5*). J. Am. Chem. Soc*., 2007, **129**: 14 176-14 177.

[69] Yang R T, Li Y W, Qi G S, et al. US Patent Applications Serial No. 2006, 11: 442898 and Serial No. 2007, 11: 820954.

[70] Li Y W, Yang R T. Significantly enhanced hydrogen storage in metal—Organic frameworks via spillover. *J. Am. Chem. Soc.*, 2006, **128**: 726-727.

[71] Li Y W, Yang R T. Hydrogen storage in metal-organic frameworks by bridged hydrogen spillover. *J. Am. Chem. Soc.*, 2006, **128**: 8136-8137.

[72] Li Y W, Yang R T. Kinetics and mechanistic model for hydrogen spillover on bridged metal-organic frameworks. *J. Phys. Chem. C*, 2007, **111**: 3405-3411.

[73] Li Y W, Yang R T. Hydrogen storage in metal-organic and covalent-organic frameworks by spillover. *AIChE J*., 2007, **54**: 269-279.

[74] Bordiga S, Vitillo J G, Richiardi G, et al. Interaction of hydrogen with MOF-5. *J. Phys. Chem. B*, 2005, **109**: 18237-8242.

[75] Yildirin T, Hartman M R. Direct observation of hydrogen adsorption sites and nanocage formation in metal-organic frameworks (MOF-5). *Phys. Rev. Lett.*, 2005, **95**: 215 504-215 507.

[76] Bordiga S, Lamberti C, Richiardi G, et al. Electronic and vibrational properties of a MOF-5 metal-organic framwwork: ZnO quantum dot behavior. *Chem. Commun*., 2004: 2300-2301.

[77] Huang L, Wang H, Chen J, et al. Synthesis, morphology control, and properties of porous metal-organic coordination polymers. *Microporous Mesoporous Mater*., 2003, **58**: 105-114.

[78] Hafizovic J, Bjørgen M, Olsbye U, et al. The inconsistency in adsorption properties and powder XRD data of MOF-5 is rationalized by framework interpenetration and the presence of organic and inorganic species in the nanocavities. *J. Am. Chem. Soc*., 2007, **129**: 3612-3620.

[79] Saha D, Yang Z, Deng S. Adsorption, equilibrium and kinetics of hydrogen in metal-organic framework (MOF)-5: Papers 255b, New Applications of Adsorption. In: AIChE Annual Meeting. Salt Lake City, USA, 2007.

[80] Saha D, Deng S. Adsorption and diffusion of gases in MOF-5, MOF-177 and zeolite 5A: Paper 132b, Applications of Adsorption and Ion Exchange. In: AIChE Annual Meeting. Philadelphia, USA, 2008.

[81] Saha D, Deng S. Adsorption equilibria and kinetics of carbon monoxide on zeolite 5A, 13X, MOF-5 and MOF-177: Paper 308a, Experimental Methods in Adsorption. In: AIChE Annual meeting. Nashville, USA, 2009.

[82] Chae H K, Siberio-Perez D Y, Kim J, et al. A route to high surface area, porosity and inclusion of large molecules in crystals. *Nature*, 2004, **427**: 523-527.

[83] Saha D. Nanoporous materials for hydrogen and carbon dioxide adsorption [Dissertation]. New Mexico State University, 2009.

[84] Rowsell J L C, Eckert J, Yaghi O M. Characterization of H_2 binding sites in prototypical metal-organic frameworks by inelastic neutron scattering. *J. Am. Soc*., 2005, **127**: 14 904-14 910.

[85] Koh K, Wong-Foy A G, Matzger A J. A crystalline mesoporous coordination copolymer with high microporosity. *Angew. Chem. Int. Ed*., 2008, **47**: 677-680.

[86] Saha D, Deng S. Synthesis and characterization and hydrogen adsorption in mixed crystals of MOF-5 and MOF-177. *Intl. J. Hydrogen Energy*, 2009, **34**: 2670-2678.

[87] Koh K, Wong-Foy A G, Matzger A J. A crystalline mesoporous, a porous coordination copolymer with over 5000 m^2/g BET surface area. *J. Am. Soc*., 2009, **131**: 4184-4185.

[88] Saha D, Wei Z, Deng S. Equilibrium, kinetics and enthalpy of hydrogen adsorption in MOF-177. *Intl. J. Hydrogen Energy*, 2008, **33**: 7479-7488.

[89] Saha D, Deng S. Structural stability of metal-organic framework (MOF)-177. *J. Phys. Chem. Lett.*, 2010, **1**: 73-78.

[90] Saha D, Deng S. Equilibrium, kinetics and enthalpy of carbon monoxide adsorption on to MOF-5, MOF-177, zeolite 5A and 13X. *J. Chem. Eng. Data*, 2009, **54**: 2245-2250.

[91] Saha D, Deng S. Adsorption equilibrium and kinetics of CO_2, CH_4 and N_2O by MOF-5, MOF-177 and zeolite 5A. *Envir. Sci. Tech*., 2010, **44**: 1820-1826.

[92] Furukawa H, Miller M A, Yaghi M. Independent verification of the saturation hydrogen uptake in MOF-177 and establishment of a benchmark for hydrogen adsorption in metal-organic frameworks. *J. Mater. Chem*., 2007, **17**: 3197-3204.

[93] Li Y, Yang R T. Gas adsorption and storage in metal-organic framework MOF-177. *Langmuir*, 2007, **23**: 12 937-12 944.

[94] Millward A R, Yaghi O M. Metal-organic frameworks with exceptionally high capacity for storage of carbon dioxide at room temperature. *J. Am. Soc*., 2005, **127**: 17 998-17 999.

[95] Wong-Foy A G, Matzger A J, Yaghi O M. Exceptional H_2 saturation uptake in microporous metal-organic frameworks. *J. Am. Soc*., 2006, **128**: 3494-3495.

[96] Tranchemontagne D J, Hunt J R, Yaghi O M. Room temperature synthesis of metal-organic frameworks: MOF-5, MOF-74, MOF-177, MOF-199, and IRMOF-0. *Tetrahedron*, 2008, **64**: 8553-8557.

[97] Caskey S R, Wong-Foy A G, Matzger A J. Phase selection and discovery among five assembly modes in a coordination polymerization. *Inorg. Chem*., 2008, **47**: 7751-7756.

[98] Li X, Cheng F, Zhang S, et al. Shape-controlled synthesis and lithium-storage study of metal-organic frameworks Zn_4O (1,3,5-benzenetribenzoate)$_2$. *J. Power Sources*, 2006, **160**: 542-547.

[99] Greathouse J A, Allendorf M D. The interaction of water with MOF-5 simulated by molecular dynamics. *J. Am. Chem. Soc*., 2006, **128**: 10 678-10 678.

[100] Poirrer E, Daily E. Thermodynamics of hydrogen adsorption in MOF-177 at low temperatures: Measurements and modeling. *Nanotechnology*, 2009, **20**: 204006 (6pp).

[101] Ruthven D M. Principles and Adsorption and Adsorption Processes. New York: Willey Interscience, 1984: 166-175.

[102] Dinca M, Long J R. Strong H_2 binding and selective gas adsorption within the microporous coordination solid Mg_3 (O_2C-$C_{10}H_6$-CO_2)$_3$. *J. Am. Soc.*, 2005, **127**: 9376-9377.